

# Anti-oxidative and anti-inflammatory effects of spirulina on rat model of non-alcoholic steatohepatitis

Wing Pak,<sup>1</sup> Fusako Takayama,<sup>1,\*</sup> Manaka Mine,<sup>1</sup> Kazuo Nakamoto,<sup>2</sup> Yasumasa Kodo,<sup>3</sup> Mitsumasa Mankura,<sup>1</sup> Toru Egashira,<sup>1</sup> Hiromu Kawasaki<sup>1</sup> and Akitane Mori<sup>1</sup>

<sup>1</sup>Graduate School of Medicine, Dentistry, and Pharmaceutical Sciences, Okayama University, 1-1-1 Tsushima-naka, Kita-ku, Okayama 700-8530, Japan

<sup>2</sup>Faculty of Pharmaceutical Sciences, Kobe Gakuin University, 1-1-3 Minatojima, Chuo-ku, Kobe 650-8586, Japan

<sup>3</sup>Spirulina Bio-Lab. Co., Ltd., 1-13-6 Nishinakajima, Yodogawa-ku, Osaka 532-0011, Japan

(Received 25 November, 2011; Accepted 20 May, 2012; Published online 12 October, 2012)

The pathogenesis of nonalcoholic steatohepatitis (NASH) remains unclear, but accumulating data suggest oxidative stress and the relationship between inflammation and immunity plays a crucial role. The aim of this study is to investigate the spirulina, which is a blue-green algae rich in proteins and other nutritional elements, and its component-phycoerythrin effect on a rat model of NASH. NASH model rats were established by feeding male Wistar rats with choline-deficient high-fat diet (CDHF) and intermittent hypoxemia by sodium nitrite challenge after 5 weeks of CDHF. After experimental period of 10 weeks, blood and liver were collected to determine oxidative stress injuries and efficacies of spirulina or phycoerythrin on NASH model rats. In the NASH model rats, increase in plasma liver enzymes and liver fibrosis, increases in productions of reactive oxygen species from liver mitochondria and from leukocytes, the activation of nuclear factor-kappa B, and the change in the lymphocyte surface antigen ratio (CD4<sup>+</sup>/CD8<sup>+</sup>) were observed. The spirulina and phycoerythrin administration significantly abated these changes. The spirulina or phycoerythrin administration to model rats of NASH might lessen the inflammatory response through anti-oxidative and anti-inflammatory mechanisms, breaking the crosstalk between oxidative stress and inflammation, and effectively inhibit NASH progression.

**Key Words:** non-alcoholic steatohepatitis, anti-oxidant, oxidative stress, anti-inflammation, spirulina

Non-alcoholic fatty liver disease has become prevalent in both developed and developing countries. Although the condition is usually considered benign, it can progress to non-alcoholic steatohepatitis (NASH), which may then lead to cirrhosis, hepatocellular carcinoma and liver failure.<sup>(1)</sup>

NASH is a progressive liver disorder that occurs in patients without significant alcohol consumption, and, histologically, it resembles the alcoholic liver disease with macrovesicular steatosis, spotty necrosis, inflammation and fibrosis.<sup>(2,3)</sup> The “two-hit theory” provides the most widely accepted explanation describing the progression of NASH. This hypothesis states that hepatic steatosis marks the first stage of NASH development. The “first hit” is considered to be related to the inflow and the increased synthesis of fatty acids, dysfunction of  $\beta$ -oxidation and obstruction of the excretion of very low density lipoprotein causing the excessive accumulation of fatty acids and neutral fat in liver hepatocytes. The “second hit” has been considered to be related to the oxidative stress caused by excess generations of reactive oxygen species (ROS) and free radicals, elevation of pro-inflammatory cytokines and appearance of mitochondrial dys-

function, all of which lead to liver inflammation and fibrosis.<sup>(4-6)</sup>

Here we describe a new and more clinically-relevant animal model of NASH (Patent application No. PCT/JP2007/52477), and demonstrated that oxidative stress causes extensive hepatic fibrosis and cirrhosis in this model rats.<sup>(7)</sup> To our knowledge, there are few published studies that have investigated the potential efficacy of antioxidant supplements against NASH progression. Information described in reports published by other groups, together with those presented in our previous papers, encourage us to select an excellent antioxidant that could potentially restrain the progression of NASH.<sup>(8-10)</sup>

Spirulina (SP, *Spirulina platensis*) is blue-green algae, contains 62% amino acids and is the world's richest natural source of vitamin B12 and contains a whole spectrum of natural mixed carotenes and xanthophyll phytopigments. SP is wrapped with a soft cell wall formed from complex sugars and proteins. Actually it is gaining more attention because of its nutritional and various medicinal properties.<sup>(11,12)</sup> SP is used as a food supplement and the nutritional and therapeutic values have been well documented.<sup>(13)</sup> SP has been claimed to possess immunomodulatory,<sup>(14)</sup> anti-oxidant,<sup>(15,16)</sup> anticancer,<sup>(17,18)</sup> antihyperlipidemic<sup>(19,20)</sup> and anti-diabetic properties<sup>(21)</sup> and shown to prevent lead toxicity.<sup>(21,22)</sup>

Phycocyanin (PC), one of the major biliproteins present in SP, is often used as a dietary nutritional supplement in many countries due to its therapeutic value, including hepatoprotective, anti-coagulant, neuroprotective and ROS-scavenging actions.<sup>(13,23-27)</sup> In addition, the anti-inflammatory activity of PC has been demonstrated in various *in vitro* studies and *in vivo* experimental models such as mice with arthritis or sepsis.<sup>(28-30)</sup>

As the antioxidative and anti-inflammatory properties of SP were expected to be able to halt the NASH progression, the present study was aimed to investigate the efficacies of SP and PC, and to elucidate their mechanisms.

## Materials and Methods

**Animals.** Male Wistar rats (Shimizu Experimental Animals, Shizuoka, Japan), weighing 160–170 g and six weeks of age were used in this study. They were housed in the Animal Research Center of Okayama University in a temperature-controlled room (22  $\pm$  1°C) with a relative humidity of 50  $\pm$  10% and a 12 h light/dark cycle (lights from 08:00 to 20:00). This study was performed in accordance with the Ethics Review Committee for Animal

\*To whom correspondence should be addressed.  
E-mail: takayamf@cc.okayama-u.ac.jp

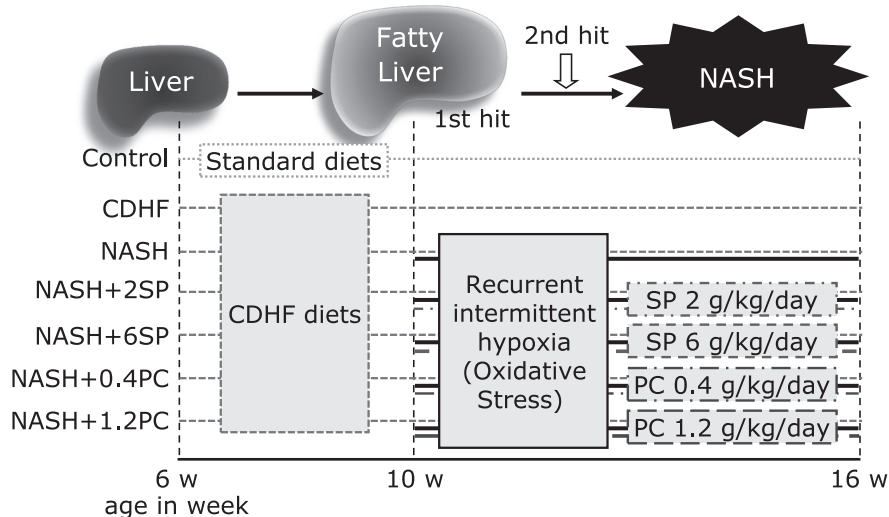


**Fig. 1.** Experimental protocol of animal experiment. In the Control group, Wistar rats were fed with standard rat chow alone for 10 weeks. The CDHF group received CDHF diet alone for 16 weeks. The NASH groups were added with injections of sodium nitrite, 50 mg/kg/day i.p., for the subsequent 6 weeks at the 10th week of continuous CDHF diets. In the NASH + 2SP and NASH + 6SP groups, spirulina, 2 g or 6 g/kg/day, was given p.o. concurrently during the period of CDHF diet and nitrite injection. In the NASH + 0.4PC and NASH + 1.2PC, the PC administration of 0.4 g or 1.2 g/kg/day was performed concurrently during the period of CDHF diet and nitrite injection.

Experimentation of the Graduate School of Medicine, Dentistry and Pharmaceutical Science, Okayama University.

**Experimental design (Fig. 1).** The rats were fed either standard chow (control group,  $n = 8$ ) for rodents (MF laboratory chow, Oriental Yeast Co., Tokyo, Japan) or choline-deficient high-fat (CDHF) diets (Oriental Yeast Co.,  $n = 48$ ) through the experiment period of 10 weeks. Fatty liver was induced by the feeding CDHF for 4 weeks. In the fifth week, rats on CDHF were divided randomly into six groups to equalize their body weight. The CDHF group ( $n = 8$ ) was fed CDHF diet only. The rest was used for the NASH model establishment,<sup>(7)</sup> and to see SP or PC effect on NASH model rats: the NASH group ( $n = 8$ ) rats were fed with CDHF diet, followed by i.p. injections of sodium nitrite ( $\text{NaNO}_2$ ), an oxidant, 50 mg/kg/day (Nacalai Tesque Inc., Kyoto, Japan) daily to induce methemoglobinemia (intermittent hypoxia stress) starting from the 5th week of CDHF for 6 weeks. In the NASH + 2SP group ( $n = 8$ ) or the NASH + 6SP group ( $n = 8$ ), SP at the dose of 2 g/kg/day or 6 g/kg/day, p.o. was given concurrently during the period of nitrite injection. In the NASH + 0.4PC group ( $n = 8$ ) or the NASH + 1.2PC group ( $n = 8$ ), PC at the dose of 0.4 g/kg/day or 1.2 g/kg/day p.o. was given concurrently during the period of nitrite injection. The PC dosage was set according to the PC content of SP.

**Blood and tissue preparation.** At the end of the 10-week experimental period, animals were sacrificed by anesthetizing with diethyl ether. Blood samples were collected by vena cava inferior puncture with syringe containing heparin, and whole body perfusion was performed to left ventricular with 0.1 M potassium chloride (Wako Pure Chem. Ind. Ltd., Osaka, Japan) containing 5 mM benzamidine (Nacalai Tesque Inc., Kyoto, Japan) before obtaining tissue samples. Plasma was obtained by centrifugation at  $1,000 \times g$  for 10 min at  $4^\circ\text{C}$ , and used for biochemical analysis.

Fresh liver was used for liver fractionation and for observation of lipid peroxidation, and a portion for histopathological observation was immersed in 10% formalin for 3 days and then embedded in paraffin. And rest of liver was rapidly frozen by liquid nitrogen, stored in  $-80^\circ\text{C}$ .

For obtaining liver fractions, six grams of liver tissue were homogenized in 18 volumes of ice-cooled 5 mM Tris-HCl buffer

(pH 7.4) containing 0.25 M sucrose (all chemicals from Wako Pure Chem. Ind. Ltd.). The mixture was centrifuged at  $700 \times g$  for 10 min at  $4^\circ\text{C}$ . The nuclear fractions were obtained and stored at  $-80^\circ\text{C}$  until analysis. The supernatant was collected and centrifuged at  $9,000 \times g$  for 20 min at  $4^\circ\text{C}$ . The resulting pellet containing the mitochondrial fraction was resuspended in the buffer and stored at  $-80^\circ\text{C}$  until analysis. The supernatant was collected and centrifuged at  $100,000 \times g$  for 60 min at  $4^\circ\text{C}$ . The resulting pellet containing the microsomal fraction was resuspended in the buffer and stored at  $-80^\circ\text{C}$  until analysis.

For obtaining liver lipid peroxidation, 55 mg of liver tissue were homogenized in 120 mM potassium chloride-30 mM phosphate buffer (pH 7.4) was centrifuged at  $450 \times g$  for 20 min at  $4^\circ\text{C}$ , supernatant samples for measurement was obtained and stored at  $-80^\circ\text{C}$  until analysis.

**Histopathological examination.** Paraffin-embedded tissues were sectioned at 4  $\mu\text{m}$  thickness and stained with Masson trichrome for fibrosis. Histological assessment of tissue morphology was performed using an Olympus light microscope (Olympus, Tokyo, Japan).

**Plasma assay for liver enzymes.** Plasma alanine aminotransferase (ALT) and aspartate aminotransferase (AST) were determined with commercial kits (Wako Pure Chem. Ind. Ltd.).

**Mitochondrial protein concentration.** Protein concentration of the liver mitochondria was determined by Lowry method.

**Derivation of ROS from liver mitochondria.** The ROS derivation from liver mitochondria was estimated by electron spin resonance (ESR) spectrometer (JES-RE1X JEOL RE-1X, JEOL, Tokyo, Japan) connected with the data analyzer (WIN-RAD, Radical Research Inc., Tokyo, Japan), using 5,5-dimethyl-1-pyrroline-1-oxide (DMPO) (Labotech Co., Tokyo, Japan) as a radical-trapping reagent.

35  $\mu\text{L}$  of mitochondria suspension in 0.25 M sucrose Tris-HCl buffer containing 0.1 M potassium chloride was mixed with 25  $\mu\text{L}$  of substrate solution containing 0.4% dodesyl maltoside, 40 mM sodium glutamate, 40 mM disodium malate and 800 mM disodium succinate in 50 mM potassium phosphate buffer, pH 7.4, 20  $\mu\text{L}$  of 4.6 M DMPO and finally 1.0 mM NADH (Oriental Yeast Co., Osaka, Japan), then was incubated at  $37^\circ\text{C}$ . After 5 min

incubation, 45  $\mu$ L aliquots of above-mentioned mixture were placed into a capillary glass tube, and this was in turn introduced into a quartz tube, and then measured at room temperature. The instrument conditions were the following: about 9.4 GHz with 100-kHz modulation frequency, central field  $\pm$  sweep width of 336.0  $\pm$  5 mT, microwave power of 8 mW, field modulation width of 0.079 mT, time constant of 0.1 s, sweep speed of 5 mT/min. The magnetic field was calculated from the splitting of divalent manganese ( $Mn^{2+}$ ), in which the distance from the third to fourth signal is 8.69 mT.

In this measurement, the characteristic ESR spectrum of the spin adducts of DMPO and hydroxyl radical (DMPO-OH) was detected. The ROS derivation was estimated by the ratio of the 2nd signal intensity of the DMPO-OH spectrum/the 3rd signal of  $Mn^{2+}$ .

**Liver lipid peroxidation assay.** The liver lipid peroxidation was determined with chemiluminescence (CL) method. 140  $\mu$ L of stored for lipid peroxidation supernatant samples were mixed with 20  $\mu$ L of 130  $\mu$ g/mL luminol (Wako Pure Chem. Ind. Ltd.) and 20  $\mu$ L of Hanks' Balanced Salt Solution (HBSS, pH 7.4), then was incubated and analyzed in the detector (TriStar LB941, Berthold Japan Co. Ltd., Tokyo, Japan) at 37°C for the baseline CL intensity. After 5 min incubation, 80  $\mu$ L of 2.2  $\mu$ g/L *tert*-butyl hydroperoxide (*tert*-BuOOH; SIGMA, St. Louis, Mo) was added. CL intensity was detected from the cleavage of lipid peroxides induced by *tert*-BuOOH addition, for 120 min with incubating at 37°C. In this measurement, lipid peroxidation levels estimated by the accumulated CL intensity by addition of *tert*-BuOOH subtract from the baseline CL intensity for 120 min.

**Leukocyte oxygen radical production.** 125  $\mu$ L of 50-fold diluted whole blood samples were mixed with 25  $\mu$ L of 300  $\mu$ g/mL luminol and 20  $\mu$ L of HBSS then was incubated at 37°C. After 5 min incubation, 80  $\mu$ L of 0.0781  $\mu$ g/mL phorbol 12-myristate 13-acetate (PMA; SIGMA) was added. The intensity of CL was estimated by measuring the amount of oxidized luminol by oxygen free radicals after PMA stimulation, as the same manner mentioned above.

**Nuclear extract and Western blot analyses to determine nuclear transcription factors.** The nuclear fractions sample suspended in 50 mM HEPES buffer (pH 7.4) containing 0.1 M potassium chloride, 3 mM magnesium chloride, 1 mM ethylenediaminetetraacetic acid, 10% Glycerol, 0.1 mM phenylmethylsulfonyl fluoride, 5  $\mu$ g/mL pepstatin A, 5  $\mu$ g/mL leupeptin and 2  $\mu$ g/mL aprotinin, and centrifuged at 22,000  $\times$  g for 20 min at 4°C. The supernatant was used as nucleoprotein samples. For protein quantification, Lowry method was used.

The nucleoprotein sample was diluted to 6 mg/mL, then mixed with sample buffer (62.5 mM Tris-HCl pH 6.8, containing 25% glycerol, 2% sodium dodecyl sulfate, 5% 2-mercaptoethanol, 0.01% bromophenol blue) and denatured at 95°C for 5 min. The samples (in 30  $\mu$ g protein/10  $\mu$ L) were separated on SDS-12.5% polyacrylamide gel (Bio-Rad Laboratories Inc., Berkeley, CA), then transferred to polyvinylidene fluoride (PVDF) membrane using a transblot apparatus (Bio-Rad Laboratories Inc.). The membranes were blocked in 5% nonfat milk dissolved in TBS-T buffer (25 mM Tris-HCl buffer, pH 7.4, containing 0.15 M sodium chloride and 0.1% Tween20) for 1 h at room temperature. The membranes were incubated with primary antibodies as follows: mouse monoclonal anti-rat nuclear factor-kappa B (NF- $\kappa$ B) (1:1000; Santa Cruz Biotechnology, Santa Cruz, CA) or rabbit polyclonal anti-rat Histone H1 (1:200; Santa Cruz Biotechnology) for 1 h. And then incubated with secondary antibodies for goat anti-mouse IgG-HRP (1:5000; Santa Cruz Biotechnology) or goat anti-rabbit IgG-HRP (1:5000; Santa Cruz Biotechnology) for 30 min. Protein bands were visualized using enhanced Chemiluminescence Luminol Reagent (Santa Cruz Biotechnology). The results were standardized by Histone H1.

**Preparation of the liver microsomal fraction.** Aliquots of liver microsomes (5  $\mu$ g) were placed in sample buffer (62.5 mM Tris-HCl pH 6.8, containing 25% glycerol, 2% sodium dodecyl sulfate, 5% 2-mercaptoethanol, 0.01% bromophenol blue) and denatured at 95°C for 5 min. Samples were separated on SDS-12.5% polyacrylamide gel and transferred to PVDF membranes, followed by Western blot analyses with the primary rabbit anti-human/rat cytochrome P450 enzyme (CYP2E1) polyclonal antibodies (1:1500; Chemicon International, Temecula, CA) or mouse monoclonal anti-rat  $\beta$ -actin (1:2000, Santa Cruz Biotechnology) for 1 h. Proteins were detected with peroxidase-conjugated secondary anti-rabbit IgG antibody or goat anti-mouse IgG HRP (1:5000; Santa Cruz Biotechnology) for 1 h and imaged using enhanced Chemiluminescence Luminol Reagent. The results were standardized by Histone H1.

**Plasma myeloperoxidase (MPO) activity.** 225  $\mu$ L of the plasma was mix with 315  $\mu$ L of 10 mM citrate buffer, pH 5.0, then aliquots of 90  $\mu$ L of these mixed liquid were pipetted into four wells. The 540 nm absorbance was monitored about the two wells to which 120  $\mu$ L of cold stop solution (4 N sulfuric acid) was added to stop the reaction to detect the background absorbance. 30  $\mu$ L of MPO substrate solution containing 6 mM 3,3',5,5'-tetramethylbenzidine dihydrochloride, 120  $\mu$ M resorcinol, and 4.4 mM hydrogen peroxide in distilled water was added to each well, and the reaction was stopped after 2 min with 120  $\mu$ L of cold stop solution, subsequently measured by absorbance at 450 nm.

As an additional control, 90  $\mu$ L of dilution buffer (without liver extract) were pipetted into four wells, 30  $\mu$ L of substrate buffer was added, followed by 120  $\mu$ L of stop solution after 2 min. No color reaction was observed in these control wells. The MPO activity of the liver sample was calculated by subtracting the mean background absorbance and is expressed as change in optical density per minute.

**Isolation of leukocytes and flow cytometry analysis of lymphocyte surface antigen CD4, CD8.** The peripheral blood was divided and erythrocytes were lysed with ammonium chloride solution, and washed twice in phosphate-buffered saline containing 0.1% sodium azide and 0.1% bovine serum albumin (BSA). The final pellet was resuspended in same buffer.

Liver tissue was dissected into 1 mm<sup>3</sup> fragments in HBSS medium containing 2% fetal bovine serum (FBS), 25 mM HEPES, 0.6% BSA, 0.125% type IV collagenase and 0.002% deoxyribonuclease I (DNase I) were added to each sample and the mixtures incubated with gentle agitation at 37°C for 30 min. Undissociated tissue was removed by filtration through a 30  $\mu$ m nylon mesh and the cells were washed twice with HBSS containing 0.001% DNase I and 25 mM HEPES with centrifugation at 250  $\times$  g for 10 min. The hepatocyte-rich matrix was removed by centrifugation for 1 min at 30  $\times$  g and the final pellet was resuspended in phosphate-buffered saline containing 0.1% sodium azide and 0.1% BSA.

For flow cytometry, the cells were incubated with fluorescein isothiocyanate (FITC) or phycoerythrin (PE)-conjugated monoclonal antibodies (antimouse CD4 [FITC], or antimouse CD8 [PE]) (all sourced from eBioscience, San Diego, CA) for 20 min, washed twice times. Then cell fixation using 400  $\mu$ L of 1% paraformaldehyde immediately before determination. At least 10,000 cells in fluorescent channel 1 for CD4, and fluorescent channel 2 for CD8 were detected using FACSCalibur<sup>TM</sup> flow cytometer (BD Biosciences, Franklin Lakes, NJ). Results were expressed as mean fluorescence intensity for a given molecule per cell.

**Statistical analyses.** Quantitative data were expressed as the mean  $\pm$  SEM of six rats. Differences among groups were examined by one-way analysis of variance (ANOVA) followed by Tukey-Kramer multiple comparison test. A value of  $p < 0.05$  was considered statistically significant.

## Results

### Histological evaluation of experimental liver samples.

The gross changes of experimental liver samples were shown in Fig. 2. The CDHF rat livers (Fig. 2b) were significantly enlarged compared to Control rats (Fig. 2a). Severe liver atrophy and cirrhosis were observed in NASH livers (Fig. 2c). The administration of SP or PC improved these changes (Fig. 2 d–g).

Masson trichrome stain was used to see fibril formation. The macrovesicular steatosis was remarkable in all zones of the liver lobe in CDHF rats (Fig. 3b). In the NASH rats, steatosis, liver fibrosis, and necrosis were quite advanced. The pseudolobule was also observed (Fig. 3c). The administration of SP or PC abated the state of the NASH (Fig. 3 d–g).

**Effects of SP or PC on plasma hepatic enzyme activities.** The plasma levels of AST and ALT were significantly higher in

**Table 1.** Effects of SP or PC on body weight and liver index

	Body weight (g)	Liver wet weight (g)	Liver index (%)
Control	366.77 ± 26.78	10.56 ± 1.93	2.88
CDHF	225.33 ± 25.74 <sup>##</sup>	11.49 ± 1.90	5.10 <sup>##</sup>
NASH	218.33 ± 24.35 <sup>##</sup>	7.35 ± 2.16	3.33
NASH + 2SP	248.13 ± 30.94 <sup>##</sup>	12.96 ± 3.41	5.22
NASH + 6SP	312.75 ± 20.25 <sup>##, **</sup>	9.54 ± 2.02	3.05 <sup>**</sup>
NASH + 0.4PC	222.33 ± 12.23 <sup>##</sup>	8.58 ± 1.84	3.84
NASH + 1.2PC	221.67 ± 22.25 <sup>##</sup>	8.57 ± 2.10	3.82

Each value denotes the mean ± SEM of 8 rats. <sup>\*\*</sup> $p < 0.01$  vs Control group; <sup>##</sup> $p < 0.01$  vs NASH group. Liver index (%): liver wet weight/body weight × 100.

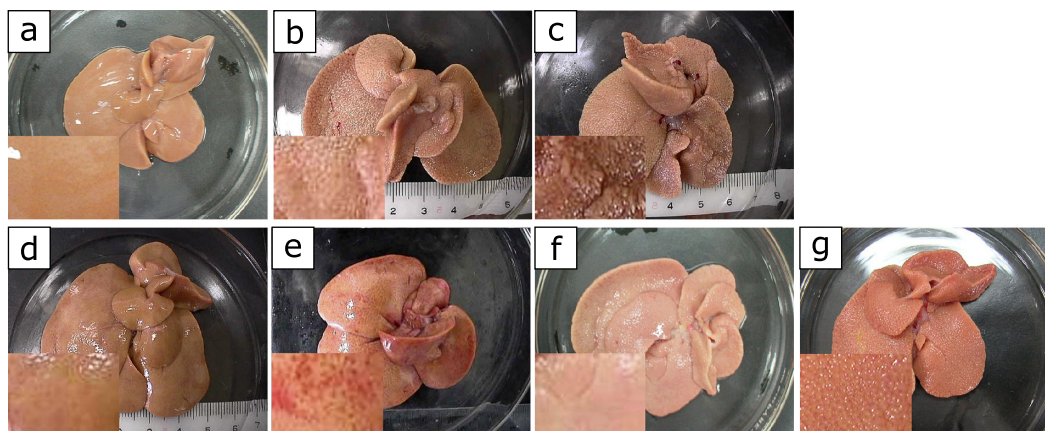


**Fig. 2.** Macroscopic views of experimental rat livers at the end of the study. See the Fig. 1 for experimental details. (a) The Control groups, (b) CDHF group, (c) NASH groups, (d) NASH + 2SP group, (e) NASH + 6SP group, (f) NASH + 0.4PC group and (g) NASH + 1.2PC group, Scale bar = 500  $\mu$ m.

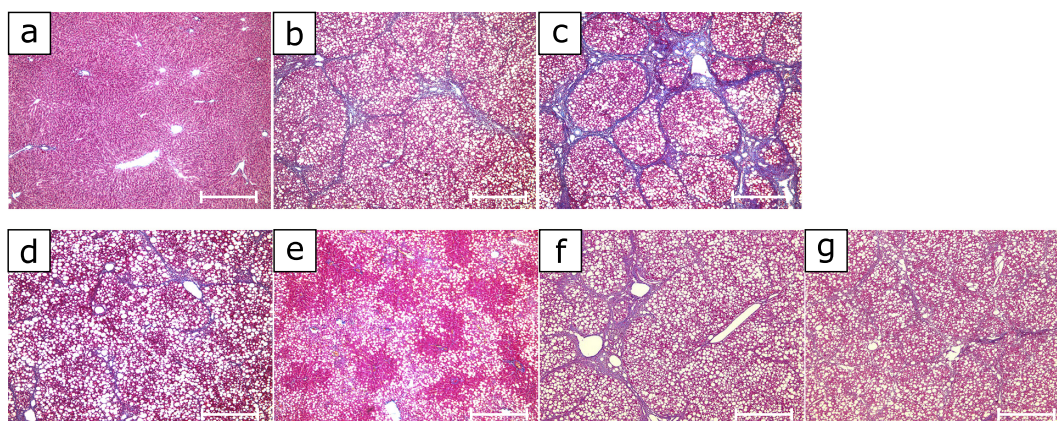


**Fig. 3.** Microscopic pictures of experimental rat livers. The experimental design is the same with Photo 1. Groups: (a) Control, (b) CDHF, (c) NASH, (d) NASH + 2SP, (e) NASH + 6SP, (f) NASH + 0.4PC and (g) NASH + 1.2PC, Scale bar = 500  $\mu$ m.

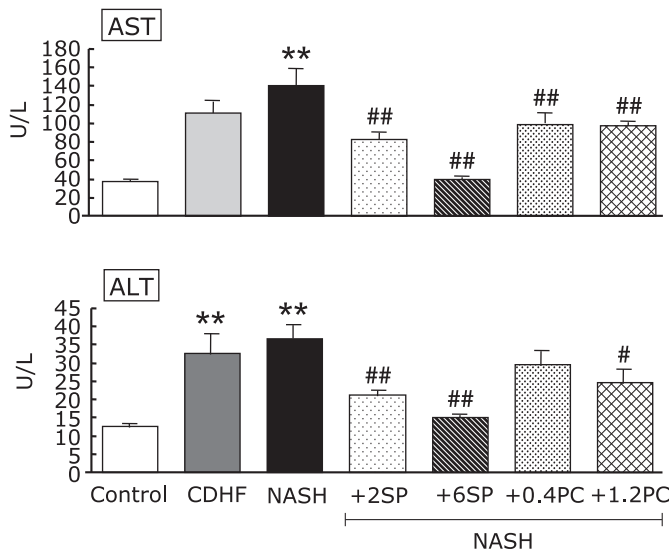


**Fig. 4.** Effects of SP or PC administration on blood hepatobiliary enzyme activities of experimental rats. Each value denotes the mean  $\pm$  SEM of 8 rats. \* $p$ <0.05, \*\* $p$ <0.01 vs Control group; # $p$ <0.05, ## $p$ <0.01 vs NASH group.

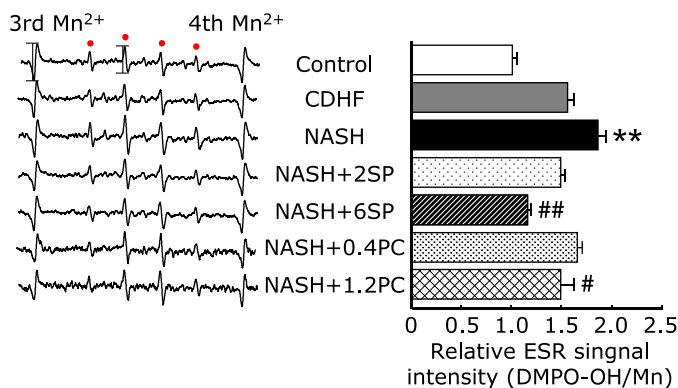


**Fig. 5.** Effects of SP or PC administration on ROS derived in the liver mitochondria of experimental rats. Each value denotes the mean  $\pm$  SEM of 8 rats. \* $p$ <0.01 vs Control group; # $p$ <0.05, ## $p$ <0.01 vs NASH group. ESR: electron spin resonance, ROS: reactive oxygen species.

NASH rats compared with rats of the Control group ( $p$ <0.01, Fig. 4). Except NASH + 0.4PC group, the administration of SP or PC to NASH rats significantly improved the AST or ALT levels compared with NASH group ( $p$ <0.05 or  $p$ <0.01).

**Effects of SP or PC on mitochondrial ROS derivation.** ROS leakage from mitochondria was evaluated by spin trapping method of ESR spectroscopy, the manganese signal as an internal standard. The amount of ROS derived from mitochondria was expressed numerically by measuring the relative peak heights of the second peaks from the DMPO-OH signals (Fig. 5). We found the highest signal intensities were obtained in NASH group. SP or PC administration caused a significant decrease in detectable levels of liver mitochondrial ROS generation compared with the NASH group ( $p$ <0.05 or  $p$ <0.01).

**Effects of SP or PC on liver lipid peroxidation.** The liver lipid peroxidation levels were significantly higher in NASH group, compared with the control group ( $p$ <0.01, Fig. 6). Administration of SP or PC was significantly prevented the lipid peroxidation of NASH rats ( $p$ <0.05).

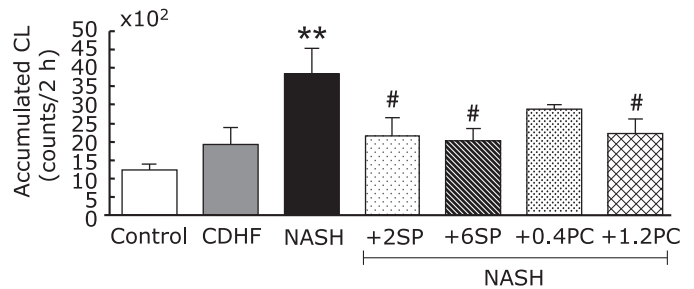


**Fig. 6.** Effects of SP or PC administration on Liver lipid peroxidation of experimental rats. Each value denotes the mean  $\pm$  SEM of 8 rats. \* $p$ <0.01 vs Control group; # $p$ <0.05 vs NASH group. CL: chemiluminescence.

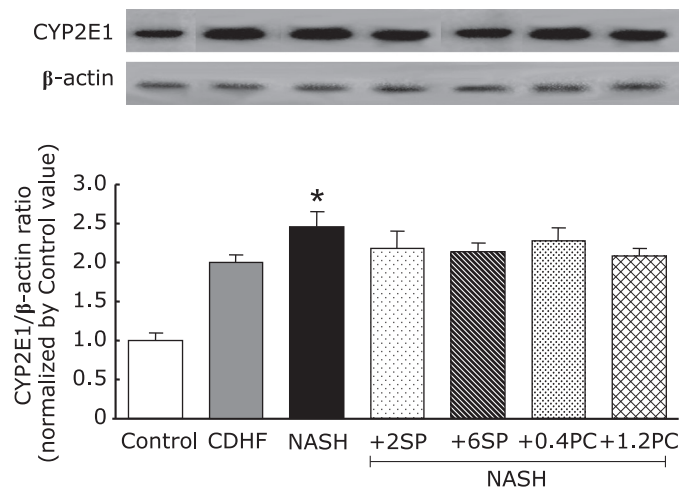


**Fig. 7.** Effects of SP or PC administration on the expression of CYP2E1 in liver of the experimental rats. Each value denotes the mean  $\pm$  SEM of 3 rats. \* $p$ <0.05 vs Control group. CYP2E1: cytochrome P450 2E1. Sample apply amounts: 30  $\mu$ g protein/10  $\mu$ L.

**Effects of VCPL on CYP2E1 induction in the liver microsomes.** The CYP2E1 expression in the NASH group was significantly higher than the control group ( $p$ <0.01, Fig. 7). However, SP or PC administration did not change the CYP2E1 expression for NASH.

**Effects of SP or PC on leukocyte ROS production.** In order to assess the state of leukocyte priming, PMA-stimulated ROS productions from leukocytes were measured (Fig. 8). In this study, CDHF and NASH groups showed significantly higher oxygen radicals signal from leukocyte compared with rats of the Control group ( $p$ <0.01). SP or PC administration, significantly suppressed ROS produced from leukocytes ( $p$ <0.05 or  $p$ <0.01).

**Effects of SP or PC on NF- $\kappa$ B activation.** NF- $\kappa$ B, a transcription factor linking between oxidative stress and inflammation, migrates to the nucleus and regulate inflammatory protein transcription when cells are activated by oxidative stress. The increase in the NF- $\kappa$ B import into nuclei of NASH rats ( $p$ <0.01, Fig. 9) is significant. SP or PC administration, significantly reduced the activation of NF- $\kappa$ B ( $p$ <0.05 or  $p$ <0.01).

**Effects of SP or PC on neutrophil activation.** Fig. 10 showed that the plasma MPO activity was significantly higher in NASH group than compared with the control group ( $p$ <0.01). Administration of SP significantly decreased plasma MPO activity ( $p$ <0.05 or  $p$ <0.01).

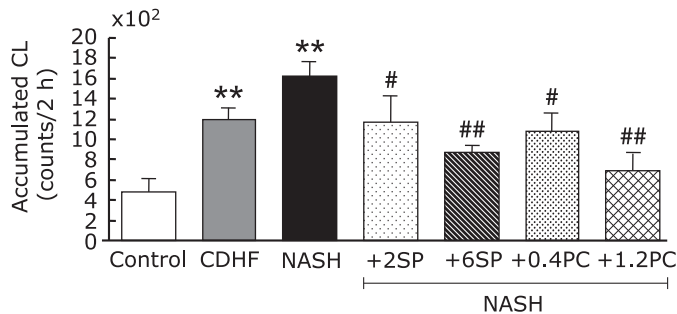


**Fig. 8.** Effects of SP or PC administration on ROS production from leukocytes of experimental rats. Each value denotes the mean ± SEM of 6 rats. \*\* $p < 0.01$  vs Control group; # $p < 0.05$ , ## $p < 0.01$  vs NASH group. ESR: electron spin resonance, ROS: reactive oxygen species, CL: chemiluminescence.

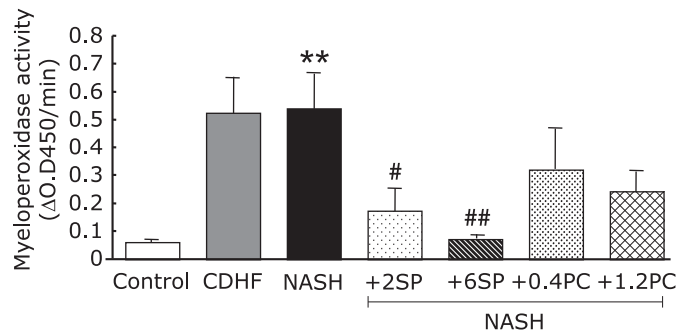


**Fig. 10.** Effects of SP or PC administration on neutrophil activation of experimental rats. Each value denotes the mean ± SEM of 8 rats. \*\* $p < 0.01$  vs Control group; # $p < 0.05$ , ## $p < 0.01$  vs NASH group.

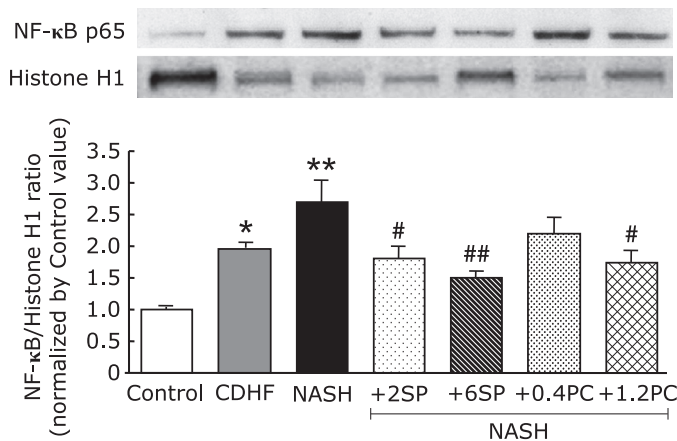


**Fig. 9.** Effects of SP or PC administration on NF-κB nuclear import in hepatocyte of experimental rats. Each value denotes the mean ± SEM of 3 rats. \*\* $p < 0.01$  vs Control group; # $p < 0.05$ , ## $p < 0.01$  vs NASH group. NF-κB: nuclear factor-kappa B. Sample apply amounts: 30 μg protein/10 μL.

#### Effects of SP or PC on Lymphocyte CD4<sup>+</sup>/CD8<sup>+</sup> ratios.

The lymphocytes CD4<sup>+</sup>/CD8<sup>+</sup> ratio of peripheral blood was significantly higher in NASH group, compared with the control group ( $p < 0.05$ , Fig. 11A), suggest the hyperactivity of immune system in NASH rats. SP or PC administration significantly decreased the ratio of CD4<sup>+</sup>/CD8<sup>+</sup> on peripheral blood ( $p < 0.05$  or  $p < 0.01$ ). Lymphocytes CD4<sup>+</sup>/CD8<sup>+</sup> ratio in liver showed no significant difference, but showed similar tendency in the peripheral blood (Fig. 11B).

#### Discussion

Recently, NASH is a very popular chronic liver disease worldwide, and it is the major cause of the elevated liver enzymes (ALT and AST in plasma) in developed countries.<sup>(31)</sup> A major problem of NASH is the lack of suitable experimental animal models. Our NASH model was developed on the basis of “Two hit theory”, and can reproduce the typical hepatic lesions of NASH, namely, steatosis, inflammation, and early fibrosis.<sup>(7)</sup> Our new rat model of NASH might be useful for understanding the disease treatment and prevention and we suggest its application as an excellent model for further mechanistic insight into NASH pathogenesis.

In the present study, we showed that administration of SP or

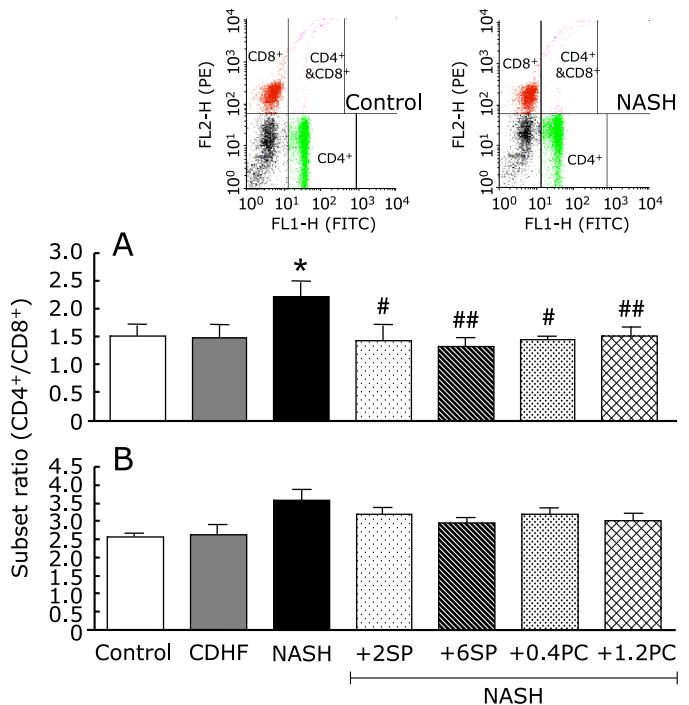


**Fig. 11.** Effects of SP or PC on Lymphocyte CD4<sup>+</sup>/CD8<sup>+</sup> ratios of experimental rats. Each value denotes the mean ± SEM of 6 rats. \* $p < 0.05$  vs Control group; # $p < 0.05$ , ## $p < 0.01$  vs NASH group.

PC improved liver atrophy, liver fibrosis and liver function (Fig. 2 and 4). We also showed that oral administration of SP or PC decreased the activities of AST and ALT in NASH rats. In a word, SP or PC successfully slowed down the development of steatohepatitis via histopathological and biochemical improvements. These effects suggest that SP or PC could play the role in protecting body against NASH.

Although the reasons for the deleterious effects of steatosis are still incompletely understood, there is growing evidence that, in the presence of oxidizable fat in the liver, ROS induces depletion of mitochondrial DNA, up-regulation of uncoupling protein 2, reduced activity of respiratory chain complexes, and impaired mitochondrial β-oxidation, resulting in mitochondrial dysfunction and abnormal mitochondrial morphology.<sup>(32,33)</sup> ROS triggered lipid peroxidation generates several reactive aldehydes. ROS and reactive aldehydes, in turn, further impair mitochondrial function, to further increase mitochondrial ROS derivation. A ROS-dependent

vicious circle may thus ensue. Therefore, the mitochondria are the most important intracellular source of ROS in NASH.<sup>(34-37)</sup> Our data also showed that the increase ROS derivation from mitochondrial and higher lipid peroxidation levels in NASH model rats liver (Fig. 5 and 6).

Some of the active constituents of SP have been reported to possess strong activity for provoking free radical scavenging enzyme system.<sup>(16,38-40)</sup> SP or PC administration in our NASH model system improved pathological changes, and this suggests that SP or PC supplementation could prevent excessive production of ROS, to regulate the balance of pro- and anti-oxidants. We, then, tried to elucidate the mechanism of SP or PC action.

CYP2E1 is a well-known other sources of oxidative stress and its levels are elevated in the liver of NASH patients.<sup>(41)</sup> Recent studies indicated that CYP2E1 plays a key role in the pathogenesis of NASH with its ability to initiate oxidative stress and increased lipid peroxidation.<sup>(42,43)</sup> Western blot analysis was used to examine the induction of CYP2E1 expression with the development of our NASH model. Our data showed higher CYP2E1 expression in the NASH model group, but SP or PC administration could not resolve these changes (Fig. 7), and higher CYP2E1 expression in our model is not associated with the progression of the disease.

It was also proposed that pro-inflammatory condition was the key predictor of eventual histological progression in NASH and could be a potential major therapeutic target.<sup>(44-46)</sup> Inflammation causes neutrophil activation and infiltration into the damaged tissues. The neutrophil infiltration may also be an important source of various pro-inflammatory mediator productions, including cytokines and oxygen-derived free radicals.<sup>(47)</sup> We observed that PMA stimulated ROS production from leukocytes were measured (Fig. 8) and SP or PC administration inhibited this inflammatory status.

NF- $\kappa$ B is known to be ubiquitously expressed and to play a major role in controlling the expression of protein involved in immune, inflammatory and acute phase response. Without stimulation, NF- $\kappa$ B is in an inactive state bound to its inhibitor I $\kappa$ B in the cytoplasm. Various agonists, such as IL-1, TNF- $\alpha$  and TLR ligands, activate NF- $\kappa$ B. Then the NF- $\kappa$ B undergoes nuclear translocation, where it binds to and stimulates transcription of target genes.<sup>(48)</sup> In this paper, the western blot analysis showed that the activation of the NF- $\kappa$ B was involved in the development of NASH (Fig. 9). The increased in MPO activity, an indicator of neutrophil activation and an important enzyme involved in the generation of reactive oxygen species,<sup>(49)</sup> was observed in NASH model (Fig. 10). SP or PC administration significantly reduced these changes, suggesting that SP could suppress NF- $\kappa$ B nuclear transport to prevent pro-inflammatory transcription and inhibit neutrophil activation.

Many of the current data show that innate immune processes both within and outside the liver are involved in NASH.<sup>(50,51)</sup> The percentages of CD4<sup>+</sup> lymphocytes and CD8<sup>+</sup> T lymphocytes and the ratio of CD4<sup>+</sup>/CD8<sup>+</sup> conveniently estimate the immune state. In this study, we measured the differentiation antigens of CD4<sup>+</sup> and CD8<sup>+</sup> in peripheral blood of NASH rats by flow cytometry to further determine the effects of SP on cellular immune function (Fig. 11). The data show that the SP can effectively normalize the immune imbalance.

In our NASH model, NaNO<sub>2</sub> was injected intraperitoneally, to provoke methemoglobinemia and decay the oxygen transport ability, which induced the intermittent hypoxemia. The enhanced oxidative stress was also demonstrated in NASH rats. So, it is firmly expected the alteration of heme oxygenase in our NASH

rats. Incidentally there is indicated that Bach1 ablation exerts hepatoprotective effect against steatohepatitis presumably via heme oxygenase induction and may be a potential therapeutic target.<sup>(52)</sup> SP efficacy would associate with the expression of Bach1 or heme oxygenase.

The present study exhibited that SP could prevent the excessive ROS derivation from the liver mitochondrial energy metabolism. Furthermore, we demonstrated that SP could relieve the ROS production from irritable inflammatory cells and the alteration of surface antigen expression of lymphocytes in the peripheral blood of NASH rats, as protective factors in liver inflammation and fibrosis. Thus, we are convinced SP also may work against NASH through anti-inflammatory and immuno-modulatory effects.

Lastly, it is well known that disturbance of lipid metabolism is a basic pathogenesis of NASH. The present study exhibited the SP efficacy against hepatic fat accumulation. Therefore, besides the anti-oxidant and anti-inflammatory activities of SP, possible metabolic roles or other mechanisms of SP in NASH rats are also considered, such as the enterobacterial flora improvement. It may play a role in ameliorating fatty liver, as the association with gut probiotic flora and attenuation of hepatic fat accumulation has been demonstrated,<sup>(53)</sup> besides reducing an inflammatory signal. However, the effect of SP on adipose metabolism needs further research.

In conclusion, we demonstrated in the present study that the anti-oxidant and anti-inflammatory activities of SP or PC can prevent the progression of NASH by normalizing the redox balance disorder and inflammatory reaction. These results not only deepen our understanding of SP, but also strongly imply that SP can be potentially used as a promising agent for prevention and therapy of NASH in clinical trials.

## Acknowledgments

We would like to express the appreciation to Pharm. M. Azusa Hasegawa and Pharm. M. Shiho Sugimoto for their kind assistance.

## Abbreviations

ALT	alanine aminotransferase
AST	aspartate aminotransferase
BSA	bovine serum albumin
CDHF	cholinedeficient high fat
CL	chemiluminescence
DMPO	5,5-Dimethyl-1-pyrroline N-oxide
FITC	fluorescein isothiocyanate
MPO	myeloperoxidase
NASH	nonalcoholic steatohepatitis
NF- $\kappa$ B	nuclear factor-kappa B
PC	phycocyanin
PE	phycoerythrin
PMA	phorbol 12-myristate 13-acetate
PVDF	polyvinylidene fluoride
ROS	reactive oxygen species
SP	spirulina
<i>tert</i> -BuOOH	<i>tert</i> -butyl hydroperoxide

## Conflict of Interest

The authors declare no conflicts of interest that are relevant to this article.

## References

- 1 Bacon BR, Farahvash MJ, Janney CG, Neuschwander-Tetri BA. Nonalcoholic steatohepatitis: an expanded clinical entity. *Gastroenterology* 1994; **107**: 1103-1109.
- 2 Ludwig J, Viggiano TR, McGill DB, Oh BJ. Nonalcoholic steatohepatitis: Mayo Clinic experiences with a hitherto unnamed disease. *Mayo Clin Proc* 1980; **55**: 434-438.

- 3 Matteoni C, Younossi ZM, Gramlich T, Boparai N, Liu YC, McCullough AJ. Nonalcoholic fatty liver disease: a spectrum of clinical and pathological severity. *Gastroenterology* 1999; **116**: 1413–1419.
- 4 Day CP, James O. Steatohepatitis: a tale of “two hits”? *Gastroenterology* 1998; **114**: 842–845.
- 5 Sanyal AJ. Nonalcoholic steatohepatitis. *Indian J Gastroenterol* 2001; **20**: 64–70.
- 6 Weltman MD, Farrell GC, Hall P, Ingelman-Sundberg M, Liddle C. Hepatic cytochrome P450 2E1 is increased in patients with nonalcoholic steatohepatitis. *Hepatology* 1998; **27**: 128–133.
- 7 Takayama F, Egashira T, Kawasaki H, et al. A novel animal model of nonalcoholic steatohepatitis (NASH): hypoxemia enhances the development of NASH. *J Clin Biochem Nutr* 2009; **45**: 335–340.
- 8 Nakamoto K, Takayama F, Mankura M, et al. Beneficial effects of fermented green tea extract in a rat model of non-alcoholic steatohepatitis. *J Clin Biochem Nutr* 2009; **44**: 239–246.
- 9 Takayama F, Nakamoto K, Kawasaki H, et al. Beneficial effects of *Vitis coignetiae* Pulliat leaves on nonalcoholic steatohepatitis in a rat model. *Acta Med Okayama* 2009; **63**: 105–111.
- 10 Takayama F, Nakamoto K, Totani N, et al. Effects of docosahexaenoic acid in an experimental rat model of nonalcoholic steatohepatitis. *J Oleo Sci* 2010; **59**: 407–414.
- 11 Ciferri O. Spirulina, the edible microorganism. *Microbiol Rev* 1983; **47**: 551–578.
- 12 Piñero Estrada JE, Bermejo Bescós P, Villar del Fresno AM. Antioxidant activity of different fractions of *Spirulina platensis* protean extract. *Farmacol* 2001; **56**: 497–500.
- 13 Kay RA. Microalgae as food and supplement. *Crit Rev Food Sci Nutr* 1991; **30**: 555–573.
- 14 Mao TK, Van de Water J, Gershwin ME. Effect of *Spirulina* on the secretion of cytokines from peripheral blood mononuclear cells. *J Med Food* 2000; **3**: 135–140.
- 15 Upasani CD, Balaraman R. Protective effect of *Spirulina* on lead induced deleterious changes in the lipid peroxidation and endogenous antioxidants in rats. *Phytother Res* 2003; **17**: 330–334.
- 16 Upasani CD, Khera A, Balaraman R. Effect of lead with vitamin E, C, or *Spirulina* on malondialdehyde, conjugated dienes and hydroperoxides in rats. *Indian J Exp Biol* 2001; **39**: 70–74.
- 17 Dasgupta T, Banejee S, Yadav PK, Rao AR. Chemomodulation of carcinogen metabolising enzymes, antioxidant profiles and skin and forestomach papillomagenesis by *Spirulina platensis*. *Mol Cell Biochem* 2001; **226**: 27–38.
- 18 Zhang HQ, Lin AP, Sun Y, Deng YM. Chemo- and radio-protective effects of polysaccharide of *Spirulina platensis* on hemopoietic system of mice and dogs. *Acta Pharmacol Sin* 2001; **22**: 1121–1124.
- 19 Iwata K, Inayama T, Kato T. Effects of *Spirulina platensis* on plasma lipoprotein lipase activity in fructose-induced hyperlipidemic rats. *J Nutr Sci Vitaminol* 1990; **36**: 165–171.
- 20 González de Rivera C, Miranda-Zamora R, Díaz-Zagoya JC, Juárez-Oropeza MA. Preventive effect of *Spirulina maxima* on the fatty liver induced by a fructose-rich diet in the rat, a preliminary report. *Life Sci* 1993; **53**: 57–61.
- 21 Parikh P, Mani U, Iyer U. Role of *Spirulina* in the control of glycemia and lipidemia in type 2 diabetes mellitus. *J Med Food* 2001; **4**: 193–199.
- 22 Shastri D, Kumar M, Kumar A. Modulation of lead toxicity by *Spirulina fusiformis*. *Phytother Res* 1999; **13**: 258–260.
- 23 Ou Y, Zheng S, Lin L, Jiang Q, Yang X. Protective effect of C-phycoerythrin against carbon tetrachloride-induced hepatocyte damage *in vitro* and *in vivo*. *Chem Biol Interact* 2010; **185**: 94–100.
- 24 Romay Ch, González R, Ledón N, Remirez D, Rimbau V. C-Phycocyanin: a biliprotein with antioxidant, anti-inflammatory and neuroprotective effects. *Curr Protein Pept Sci* 2003; **4**: 207–216.
- 25 Vadiraja BB, Gaijwad NW, Madyastha KM. Hepatoprotective effect of C-phycoerythrin: protection for carbon tetrachloride and R-(+)-pulegone-mediated hepatotoxicity in rats. *Biochem Biophys Res Commun* 1998; **249**: 428–431.
- 26 Bhat VB, Madyastha KM. C-phycoerythrin: a potent peroxyl radical scavenger *in vivo* and *in vitro*. *Biochem Biophys Res Commun* 2000; **275**: 20–25.
- 27 Chiu HF, Yang SP, Kuo YL, Lai YS, Chou TC. Mechanisms involved in the antiplatelet effect of C-phycoerythrin. *Br J Nutr* 2006; **95**: 435–440.
- 28 Romay C, Armesto J, Remirez D, González R, Ledón N, García I. Antioxidant and anti-inflammatory properties of C-phycoerythrin from blue-green algae. *Inflamm Res* 1998; **47**: 36–41.
- 29 Remirez D, González R, Merino N, Rodríguez S, Ancheta O. Inhibitory effects of *Spirulina* in zymosan-induced arthritis in mice. *Mediators Inflamm* 2002; **11**: 75–79.
- 30 Romay C, Delgado R, Remirez D, González R, Rojas A. Effects of phycoerythrin extract on tumor necrosis factor- $\alpha$  and nitrite levels in serum of mice treated with endotoxin. *Arzneimittelforschung* 2001; **51**: 733–736.
- 31 Clark JM, Brancati FL, Diehl AM. The prevalence and etiology of elevated aminotransferase levels in the United States. *Am J Gastroenterol* 2003; **98**: 960–967.
- 32 Pessayre D, Mansouri A, Fromenty B. Nonalcoholic steatosis and steatohepatitis. V. Mitochondrial dysfunction in steatohepatitis. *Am J Physiol Gastrointest Liver Physiol* 2002; **282**: G193–G199.
- 33 Browning JD, Horton JD. Molecular mediators of hepatic steatosis and liver injury. *J Clin Invest* 2004; **114**: 147–152.
- 34 Fromenty B, Robin MA, Igoudjil A, Mansouri A, Pessayre D. The ins and outs of mitochondrial dysfunction in NASH. *Diabetes Metab* 2004; **30**: 121–138.
- 35 Caldwell SH, Swerdlow RH, Khan EM, et al. Mitochondrial abnormalities in non-alcoholic steatohepatitis. *J Hepatol* 1999; **31**: 430–434.
- 36 Begriche K, Igoudjil A, Pessayre D, Fromenty B. Mitochondrial dysfunction in NASH: causes, consequences and possible means to prevent it. *Mitochondrion* 2006; **6**: 1–28.
- 37 Wei Y, Rector RS, Thyfault JP, Ibdah JA. Nonalcoholic fatty liver disease and mitochondrial dysfunction. *World J Gastroenterol* 2008; **14**: 193–199.
- 38 Mathew B, Sankaranarayanan R, Nair PP, et al. Evaluation of chemoprevention of oral cancer with *Spirulina fusiformis*. *Nutr Cancer* 1995; **24**: 197–202.
- 39 Miranda MS, Cintra RG, Barros SB, Mancini Filho J. Antioxidant activity of the microalga *Spirulina maxima*. *Braz J Med Biol Res* 1998; **31**: 1075–1079.
- 40 Premkumar K, Pachiappan A, Abraham SK, Santhiya ST, Gopinath PM, Ramesh A. Effect of *Spirulina fusiformis* on cyclophosphamide and mitomycin-C induced genotoxicity and oxidative stress in mice. *Fitoterapia* 2001; **72**: 906–911.
- 41 Weltman MD, Farrell GC, Hall P, Ingelman-Sundberg M, Liddle C. Hepatic cytochrome P450 2E1 is increased in patients with nonalcoholic steatohepatitis. *Hepatology* 1998; **27**: 128–133.
- 42 Robertson G, Leclercq I, Farrell GC. Nonalcoholic steatosis and steatohepatitis. II. Cytochrome P-450 enzymes and oxidative stress. *Am J Physiol Gastrointest Liver Physiol* 2001; **281**: G1135–G1139.
- 43 Leclercq IA, Farrell GC, Field J, Bell DR, Gonzalez FJ, Robertson GR. CYP2E1 and CYP4A as microsomal catalysts of lipid peroxides in murine nonalcoholic steatohepatitis. *J Clin Invest* 2000; **105**: 1067–1075.
- 44 Reddy JK, Rao MS. Lipid metabolism and liver inflammation. II. Fatty liver disease and fatty acid oxidation. *Am J Physiol Gastrointest Liver Physiol* 2006; **290**: G852–G858.
- 45 Shoelson SE, Herrero L, Naaz A. Obesity, inflammation, and insulin resistance. *Gastroenterology* 2007; **132**: 2169–2180.
- 46 Day CP. From fat to inflammation. *Gastroenterology* 2006; **130**: 207–210.
- 47 Fantone JC, Ward PA. Role of oxygen-derived free radicals and metabolites in leukocyte-dependent inflammatory reactions. *Am J Pathol* 1982; **107**: 395–418.
- 48 Tian B, Brasier AR. Identification of a nuclear factor  $\kappa$ B-dependent gene network. *Recent Prog Horm Res* 2003; **58**: 95–130.
- 49 Klebanoff SJ. Myeloperoxidase: friend and foe. *J Leukoc Biol* 2005; **77**: 598–625.
- 50 Maher JJ, Leon P, Ryan JC. Beyond insulin resistance: innate immunity in nonalcoholic steatohepatitis. *Hepatology* 2008; **48**: 670–678.
- 51 Zhan YT, An W. Roles of liver innate immune cells in nonalcoholic fatty liver disease. *World J Gastroenterol* 2010; **37**: 4652–4660.
- 52 Xu RY, Wan YP, Fang QY, Lu W, Cai W. Supplementation with probiotics modifies gut flora and attenuates liver fat accumulation in rat nonalcoholic fatty liver disease model. *J Clin Biochem Nutr* 2012; **50**: 72–77.
- 53 Inoue M, Tazuma S, Kanno K, Hyogo H, Igarashi K, Chayama K. Bach1 gene ablation reduces steatohepatitis in mouse MCD diet model. *J Clin Biochem Nutr* 2011; **48**: 161–166.